



This paper is a part of the hereunder thematic dossier published in OGST Journal, Vol. 70, No. 1, pp. 3-211 and available online [here](#)

Cet article fait partie du dossier thématique ci-dessous publié dans la revue OGST, Vol. 70, n°1, pp. 3-211 et téléchargeable [ici](#)

DOSSIER Edited by/Sous la direction de : **B. Leduc et P. Tona**

IFP Energies nouvelles International Conference / Les Rencontres Scientifiques d'IFP Energies nouvelles
E-COSM'12 — IFAC Workshop on Engine and Powertrain Control, Simulation and Modeling
E-COSM'12 — Séminaire de l'IFAC sur le contrôle, la simulation et la modélisation des moteurs
et groupes moto-propulseurs

Oil & Gas Science and Technology – Rev. IFP Energies nouvelles, Vol. 70 (2015), No. 1, pp. 3-211

Copyright © 2015, IFP Energies nouvelles

- 3 > Editorial
B. Leduc and P. Tona
- 15 > *A Challenging Future for the IC Engine: New Technologies and the Control Role*
Un challenge pour le futur du moteur à combustion interne : nouvelles technologies et rôle du contrôle moteur
F. Payri, J. M. Luján, C. Guardiola and B. Pla
- 31 > *The Art of Control Engineering: Science Meets Industrial Reality*
L'art du génie automatique : science en rencontre avec la réalité industrielle
U. Christen and R. Busch
- 41 > *Energy Management of Hybrid Electric Vehicles: 15 Years of Development at the Ohio State University*
Gestion énergétique des véhicules hybrides électriques : 15 ans de développement à l'université d'État de l'Ohio
G. Rizzoni and S. Onori
- 55 > *Automotive Catalyst State Diagnosis using Microwaves*
Diagnostic de l'état de catalyseurs d'automobiles à l'aide de micro-ondes
R. Moos and G. Fischerauer
- 67 > *Control-Oriented Models for Real-Time Simulation of Automotive Transmission Systems*
Modélisation orientée-contrôle pour la simulation en temps réel des systèmes de transmission automobile
N. Cavina, E. Corti, F. Marcigliano, D. Olivi and L. Poggio
- 91 > *Combustion Noise and Pollutants Prediction for Injection Pattern and Exhaust Gas Recirculation Tuning in an Automotive Common-Rail Diesel Engine*
Prédiction du bruit de combustion et des polluants pour le réglage des paramètres d'injection et de l'EGR (*Exhaust Gas Recirculation*) dans un moteur Diesel *Common-Rail* pour l'automobile
I. Arsie, R. Di Leo, C. Pianese and M. De Cesare
- 111 > *Investigation of Cycle-to-Cycle Variability of NO in Homogeneous Combustion*
Enquête de la variabilité cycle-à-cycle du NO dans la combustion homogène
A. Karvountzis-Kontakiotis and L. Ntziachristos
- 125 > *Energy Management Strategies for Diesel Hybrid Electric Vehicle*
Lois de gestion de l'énergie pour le véhicule hybride Diesel
O. Grondin, L. Thibault and C. Quérel
- 143 > *Integrated Energy and Emission Management for Diesel Engines with Waste Heat Recovery Using Dynamic Models*
Une stratégie intégrée de gestion des émissions et de l'énergie pour un moteur Diesel avec un système WHR (*Waste Heat Recovery*)
F. Willems, F. Kupper, G. Rascanu and E. Feru
- 159 > *Development of Look-Ahead Controller Concepts for a Wheel Loader Application*
Développement de concepts d'une commande prédictive, destinée à une application pour chargeur sur pneus
T. Nilsson, A. Fröberg and J. Åslund
- 179 > *Design Methodology of Camshaft Driven Charge Valves for Pneumatic Engine Starts*
Méthodologie pour le design des valves de chargement opérées par arbre à cames
M.M. Moser, C. Voser, C.H. Onder and L. Guzzella
- 195 > *Design and Evaluation of Energy Management using Map-Based ECMS for the PHEV Benchmark*
Conception et évaluation de la gestion de l'énergie en utilisant l'ECMS (stratégie de minimisation de la consommation équivalente) basée sur des cartes, afin de tester les véhicules hybrides électriques rechargeables
M. Sivertsson and L. Eriksson

Investigation of Cycle-to-Cycle Variability of NO in Homogeneous Combustion

A. Karvountzis-Kontakiotis and L. Ntziachristos*

Aristotle University of Thessaloniki, Laboratory of Applied Thermodynamics (LAT), GR54125, POB 458, Thessaloniki, Greece
e-mail: akarvout@auth.gr - leon@auth.gr

* Corresponding author

Abstract — *Cyclic variability of spark ignition engines is recognized as a scatter in the combustion parameter recordings during actual operation in steady state conditions. Combustion variability may occur due to fluctuations in both early flame kernel development and in turbulent flame propagation with an impact on fuel consumption and emissions. In this study, a detailed chemistry model for the prediction of NO formation in homogeneous engine conditions is presented. The Wiebe parameterization is used for the prediction of heat release; then the calculated thermodynamic data are fed into the chemistry model to predict NO evolution at each degree of crank angle. Experimental data obtained from literature studies were used to validate the mean NO levels calculated. Then the model was applied to predict the impact of cyclic variability on mean NO and the amplitude of its variation. The cyclic variability was simulated by introducing random perturbations, which followed a normal distribution, to the Wiebe function parameters. The results of this approach show that the model proposed better predicts mean NO formation than earlier methods. Also, it shows that to the non linear formation rate of NO with temperature, cycle-to-cycle variation leads to higher mean NO emission levels than what one would predict without taking cyclic variation into account.*

Résumé — **Enquête de la variabilité cycle-à-cycle du NO dans la combustion homogène** — La variabilité cyclique des moteurs à allumage commandé est reconnue comme une dispersion dans les enregistrements des paramètres de combustion lors du fonctionnement réel dans des conditions stables. Des variabilités de combustion peuvent se produire en raison des fluctuations dans le développement précoce du noyau de la flamme et dans la propagation turbulente de la flamme avec un impact sur la consommation de carburant et les émissions. Cette étude présente un modèle chimique détaillé pour prévoir la formation de NO dans des conditions de combustion homogène. Le paramétrage de Wiebe est utilisé pour prévoir le dégagement de chaleur ; les données thermodynamiques calculées sont ensuite intégrées au modèle chimique pour prévoir l'évolution de NO à chaque degré d'angle de rotation du vilebrequin. Les données expérimentales obtenues à partir de l'analyse des publications antérieures ont été utilisées pour valider les niveaux moyens de NO calculés. Le modèle a ensuite été appliqué pour prévoir l'impact de la variabilité cyclique sur le taux moyen de NO formé et l'amplitude de sa variation. La variabilité cyclique a été simulée en introduisant des perturbations aléatoires qui suivent une distribution normale, aux paramètres de la fonction de Wiebe. Les résultats de cette approche montrent que le modèle proposé prédit mieux le taux moyen de formation de NO que les méthodes précédentes. Les résultats montrent également

qu'une vitesse de formation non linéaire de NO avec la température et la variation cycle-à-cycle, entraîne une moyenne plus élevée des niveaux d'émission de NO que celle prédite sans prendre en compte la variation cyclique.

NOMENCLATURE

ABDC	After Bottom Dead Centre
ATDC	After Top Dead Centre
BBDC	Before Bottom Dead Centre
BTDC	Before Top Dead Centre
CCV	Cycle to Cycle Variation
CD	Combustion Duration
CFD	Computational Fluid Dynamics
COV	Coefficient Of Variation
EVC	Exhaust Valve Close
EVO	Exhaust Valve Open
imep	indicated mean effective pressure
IVC	Intake Valve Close
IVO	Intake Valve Open
m	Wiebe shape coefficient
MC	Mean Cycle
PL	Partial Load
SD	Standard Deviation
SI	Spark Ignition
SOI	Start Of Ignition
WOT	Wide Open Throttle

INTRODUCTION

Combustion in engines evolves differently in each operation cycle even at steady state operating conditions. Experimentally, Cycle-to-Cycle Variability (CCV) is best observed by the scatter of the measured cylinder pressure around the mean pressure curve. Such fluctuations of the cylinder pressure have an impact on engine performance [1], fuel consumption [2] and pollutant emissions [3, 4], while in some extreme cases such as highly diluted lean mixtures could result in misfiring or knocking [2]. The Coefficient Of Variation of the indicated mean effective pressure (COV_{imep}) is used for the classification of CCV [5]. In general, COV_{imep} should be limited to up to about 10% in order to avoid vehicle drivability problems [5, 6].

There are several reasons that may cause CCV. These may include variations in the early flame kernel development due to corresponding spark variance in each cycle or the turbulence conditions in the spark neighbourhood. The kernel development affects flame propagation, which by turn results to different macroscopic combustion parameters. The spark discharge

characteristics [2], the local equivalence ratio of the mixture and its inhomogeneity close to the spark plug [2, 7, 8], turbulence in the vicinity of spark plug at the ignition time [8], and mixture temperature and pressure at the time of ignition [8] are all related with the variations of the early flame kernel development. On the other hand, the overall equivalence ratio [9], the extent of mixture homogeneity [10, 11], the percentage of the residual gas fraction of the mixture [10] and the averaged turbulence intensity [12-16] are factors that affect the main flame propagation.

Combustion CCV also leads to variability in the combustion products. NO_x formation in particular shows a strong dependence on combustion duration. NO_x emissions decrease as combustion time decreases and this dependence becomes stronger as air-fuel ratio becomes leaner [17]. In other studies, it was found that the variance of NO_x is higher compared with the variance of imep and the maximum combustion pressure [3, 18].

There have been several model approaches aiming at simulating combustion development and pollutants formation in SI engines. The Wiebe function [19] has been applied in most studies for the approximation of heat release due to fuel consumption. However this empirical function does not have a physical meaning and its predictability is not always satisfactory. Zero-dimensional phenomenological models may better approach the actual physics, taking into account different temperature zones and compositions. However the turbulence conditions in the combustion chamber cannot be modeled with this kind of models [20], hence they cannot be used to simulate CCV. As a result, CFD models (1D/3D) are mainly used for the simulation of CCV, because they are able to precisely simulate both the rate of the early flame development and the flame propagation [12, 13, 21, 22]. Their disadvantage is their high computational cost and the difficulty in setting up a satisfactory combustion CFD model [20].

In SI modeling, NO emissions are usually simulated by applying the extended Zeldovich mechanism, also known as the thermal mechanism [23, 24]. However, in stoichiometric and slightly rich mixtures, the prompt (also known as Fenimore) mechanism could be responsible for up to fifteen percent of the total nitric oxide emissions [25].

The objective of this study is the investigation of the combustion CCV in nitric oxide emissions, using a detailed chemical mechanism. The simple two-zone

Wiebe model is used for the description of the mixture temperature and pressure during combustion. The thermodynamic parameters for each cycle are used as input in the detailed chemical mechanism for the prediction of NO formation as a function of degree of crank angle. The model is then used to predict the impact of CCV on NO emission levels.

1 MODEL APPROACH

The model presented in this paper consists of a detailed chemical mechanism, coupled to a two zone Wiebe model [19, 23]. For the aim of this study, the three parameters of the Wiebe function were individually perturbed around central values to simulate CCV, thus having an impact on the burning rate and the NO formation.

1.1 Thermodynamic Model

The commercial engine simulation package AVL BOOST was used for the simulation of the heat release rate and the in-cylinder thermodynamic properties. The combustion submodel used for the prediction of heat release was a two-zone Wiebe model. The Wiebe function describes the burned gas mass fraction at a given crank angle:

$$\frac{Q_f(\phi)}{Q_{f,total}} = 1 - e^{-\alpha \left(\frac{\phi - \phi_{SOI}}{\Delta\phi_{CD}} \right)^{m+1}} \quad (1)$$

In Equation (1), ϕ_{SOI} is the degree of crank angle where ignition starts, $\Delta\phi_{CD}$ is the duration of combustion in crank angle degrees, m is a shape parameter for the Wiebe function, and α is a combustion efficiency parameter.

The two-zone approach consists of a burned zone with a temperature for the combustion products and an unburned zone with a different temperature for the unburned mixture and any residuals from the previous combustion cycle. A uniform pressure for both zones is assumed. Although the Wiebe model is an empirical model and it is not recommended for the investigation of the CCV origins, variation of its parameters provides a good approximation in simulating combustion exothermy variability.

1.2 Emission Model

The chemistry model used to predict NO formation was based on SENKIN, a FORTRAN based code developed in Sandia Laboratories [26] that has been later evolved

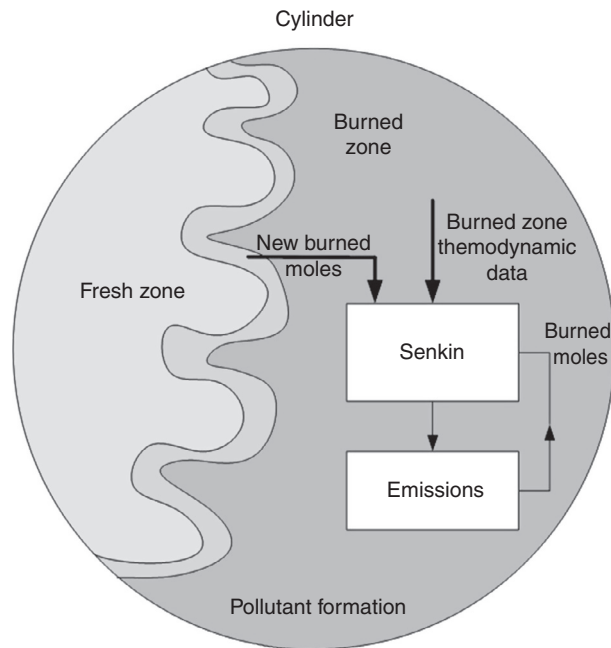


Figure 1
Schematic of the emission modeling approach.

into the CHEMKIN software package. SENKIN calculates combustion evolution in homogeneous gas phase mixtures. The code solves the chemical kinetics differential equations and predicts the formation rate of products. This solution can refer either to constant pressure, constant volume, or constant temperature conditions. The default reaction scheme of SENKIN v1.8 that was used in this study, consisted of 53 species and 325 chemical reactions [26, 27]. The reaction scheme involved of a number of carbon-nitrogen species and radicals which are relevant in the NO formation chemistry, including HCN, H₂CN, CN, HCNO and HOCN.

Figure 1 illustrates the coupling between the thermodynamic and the chemical kinetic modeling developed in the current study. The thermodynamic data for the hot zone are imported in the converter at each crank angle. The burned mass fraction from the Wiebe function defines the newly burned moles which enter from the flame front to the burned zone. The newly burned moles are calculated from the oxidation rate of the fuel, according to the stoichiometry of the combustion shown in Table 1.

The newly burned moles and the composition from the previous step are imported as the initial input composition of the burned zone in SENKIN. SENKIN calculates as an output the new composition of the burned zone which will be again imported in the next crank angle.

When the thermodynamic model calculates the end of combustion, no new moles are assumed in the SENKIN input scenario. The loop therefore ends and kinetics are thereafter considered frozen. In earlier typical two zone models [18, 22, 23, 28] only the thermal mechanism was considered, while the other necessary species for the thermal mechanism (H_2 , H , O_2 , O , OH , H_2O) were calculated assuming equilibrium. The proposed emission model uses a detailed chemical mechanism which includes the thermal and the prompt mechanism, while the other necessary species are calculated from detailed kinetics. This improves the precision in NO_x prediction, with a cost in computational time. A reduced detailed chemical mechanism but with explicit kinetics for intermediate species could serve as a compromise between accuracy and computational time.

1.3 Modeling of NO CCV

The modeling of NO CCV was performed by introducing perturbations into the Wiebe function parameters, regarding the ignition timing (SOI), the Combustion Duration (CD) and the parameter m . Each of these three parameters was described by a normal distribution, characterized by a mean value and a standard deviation. The mean value of each distribution was the Wiebe value of the mean-cycle model, while the range of perturbations was taken from experimental data, as it will be later discussed. Finally the CCV thermodynamic data were imported in the detailed chemical mechanism. This procedure was modeled in MATLAB.

1.4 Modeling Assumptions

The following assumptions were considered for the simplification of the emission modeling and the CCV analysis:

- uniform pressure in the cylinder (burned and unburned zone at the same pressure);

TABLE 1

The new species imported in the emission model at each iteration, assuming C_aH_b as the chemical formula of the hydrocarbon fuel

Species	$\lambda \geq 1$	$0.9 < \lambda < 1$
CO_2	a	$a \cdot (2\lambda - 1) + b/2 \cdot (\lambda - 1)$
H_2O	$b/2$	$b/2$
CO	0	$(2a + b/2) \cdot (1 - \lambda)$
O_2	$(2a + b/2) \cdot (\lambda - 1)$	0
N_2	$3.76 \cdot \lambda \cdot (a + b/4)$	$3.76 \cdot \lambda \cdot \alpha s$

- a complete combustion of hydrocarbon fuel with air;
- uniform composition in the burned zone;
- NO_x emissions solely consisting of NO .

The validity and impact of these assumptions in the final results is investigated in the results section.

2 EXPERIMENTAL DATA

Experimental data are necessary for the validation of the model developed in this study. In most CCV analysis, only the thermodynamic data are measured, without considering the emission data. Ball *et al.* (1998) [4] used experimental data from a *Rover K4* optical engine to investigate cycle-to-cycle variation in combustion and NO emissions. The fuel used in those experiments was methane. That engine from the Ball *et al.* (1998) [4] work was simulated in the present study, as many engine specifications necessary for the modeling are contained in that publication and are summarized in Table 2. The model was applied to this engine and the results of the

TABLE 2

The *Rover K4* optical engine characteristics (Ball *et al.*, 1998) [4]

Main specification		
Bore	80	(mm)
Stroke	89	(mm)
ConRod length	160	(mm)
Compression ratio	10	(-)
Cam timing		
IVO	12	BTDC
IVC	52	ABDC
Peak lift inlet	8.8	(mm) at 70 BBDC
EVO	52	BBDC
EVC	12	ATDC
Peak lift exhaust	8.8	(mm) at 70 ABDC
Cylinder head		
Type		Rover K16 1.4 MPI
Pent angle	45	
Inlet valve seat diameter	24	(mm)
Inlet valve seat diameter	19.6	(mm)
Number of valves	4	(-)

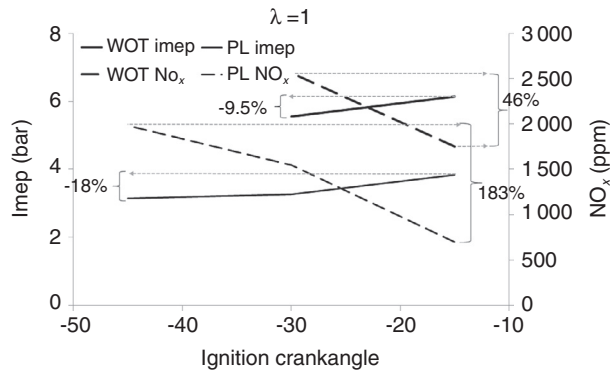


Figure 2
Effect of the ignition timing on imep and NO_x for stoichiometric conditions.

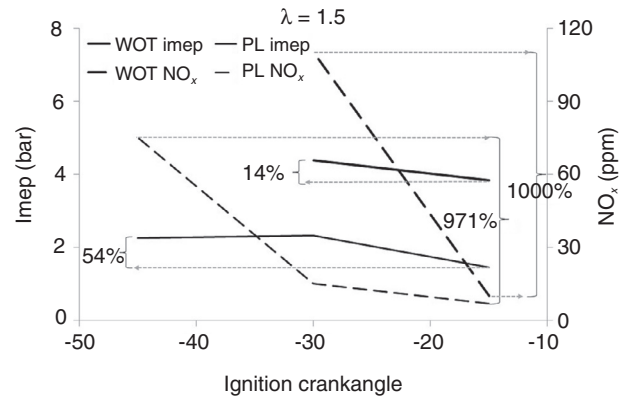


Figure 3
Effect of ignition timing on imep and NO_x for lean conditions.

simulations were compared with the experimental data for validation.

This optical engine was measured under partial load and Wide Open Throttle conditions (WOT), for different crank angle ignition durations and lambda values. Information about the engine performance and the engine emissions (NO_x, HC) was also available for each measured engine point.

3 EFFECT OF ENGINE OPERATION PARAMETERS ON EMISSIONS

Based on the experimental data presented in the previous section, Figure 2 presents a graph of imep and NO_x concentration for stoichiometric combustion, during Partial Load (PL) and WOT operation. It is observed that while the Start Of Ignition (SOI) changed from 15° BTDC to 45° BTDC partial load imep only differed by 18%, the WOT imep differed by 9.5%, while NO_x concentrations changed by 183% and 46%, respectively. This shows how much more sensitive NO formation is than the thermodynamic properties of the engine when combustion parameters change.

The corresponding graph for lean operation ($\lambda = 1.5$) is shown in Figure 3. The impact of the variation in combustion parameters on NO_x formation is even more magnified in this case compared to the stoichiometric combustion.

By comparing the two cases, it is observed that in lean operating conditions, the impact of the ignition timing on the indicated mean effective pressure is higher compared to the stoichiometric mixture, an observation which is in agreement with other studies [2-9]. From these data it seems that cycle-to-cycle combustion

variability is more pronounced in lean and highly diluted mixtures, even with slight modification of the combustion parameters. In addition such conditions lead to high NO_x formation, hence the CCV effect is magnified in this case as well.

This non-linearity of NO_x formation is not easy to simulate in detail with a simplified mechanism. Hence, a detailed and more precise chemical mechanism is applied in this study, in order to simulate this non-linearity and high sensitivity in NO_x formation. The model presented in this study can be used to predict the amplitude of variation of NO_x emissions due to CCV and, in this way, to more accurately predict the compliance of an engine with a given emission limit target.

4 RESULTS

For validation, the proposed emission model is first used to predict the *Rover K4* NO_x measured emissions at both stoichiometric and lean conditions. First, the measured data of *Rover K4* are used regarding NO_x emissions and engine performance characteristics to relate the tendency between performance and emissions. Second, the comparison between simulated and experimental cycle-averaged NO data is presented for the validation of the simulation. Measurement and simulation are discussed and the importance of the prompt NO formation mechanism is justified. Last but not least, the NO CCV is investigated.

4.1 Mean Cycle NO Modeling

The *Rover K4* was simulated with the AVL BOOST model for mean cycle Wiebe parameters and the results

TABLE 3
Validation of the thermodynamic model

Case	λ	θ_{ign} (BTDC)	Imep (bar)	P_{max} (bar)	CaPmax (ATDC)	10% MFB (ATDC)
Part load						
P1015 exp	1	15	3.84	18.05	20	5
P1015 sim	1	15	3.84	16.45	20.11	4.94
P1030 exp	1	30	3.27	25.92	7	-10
P1030 sim	1	30	3.27	20.47	10.92	-11.42
P1045 exp	1	45	3.15	29.34	2	-18
P1045 sim	1	45	3.14	32.37	3.07	-18.32
P1515 exp	1.5	15	1.46	10.23	0	19
P1515 sim	1.5	15	1.44	12.2	1.34	19.37
P1530 exp	1.5	30	2.33	15.13	12	-2
P1530 sim	1.5	30	2.33	14.96	11.84	-2.24
P1545 exp	1.5	45	2.25	21.44	6	-16
P1545 sim	1.5	45	2.23	25.48	6.26	-15.91
WOT						
W1015 exp	1	15	6.14	33.02	18	3
W1015 sim	1	15	6.15	35.76	19.99	2.27
W1030 exp	1	30	5.55	45.68	5	-11
W1030 sim	1	30	5.55	55.34	7.45	-11.18
W1515 exp	1.5	15	3.83	17.33	10	11
W1515 sim	1.5	15	3.82	21.07	3.51	10
W1530 exp	1.5	30	4.38	29.2	12	-3
W1530 sim	1.5	30	4.38	29.67	13.83	-3.23

were compared with the experimental cycle-averaged engine data found in Ball *et al.* (1998) [4]. The comparison between experimental and simulated data refers to the imep, the maximum pressure during the combustion phase, the crank-angle degree where maximum pressure occurs, and the crank angle degree where 10% of the fuel mass is burned (MFR). All these data are presented in Table 3. The designation of each point in Table 3 is done with the P and W initials corresponding to partial load or wide open throttle operation, respectively, followed by two digits corresponding to the lambda value (10 corresponding to $\lambda = 1$ and 15 corresponding to $\lambda = 1.5$), followed by two digits of crank angle degree where ignition starts before top dead centre.

The predicted thermodynamic data of the ten simulated operating points were used as an input for the NO prediction. The simulated NO emissions are compared with the experimental NO emissions in Figure 4 for stoichiometric combustion and in Figure 5 for the lean combustion. In the stoichiometric combustion, NO emissions are presented with and without the effect of the prompt mechanism. The prompt mechanism has been switched off by zeroing the HCN radicals in the chemical mechanism.

The model appears to have a rather good accuracy over a wide NO_x range, that is from NO_x concentrations of less than 10 ppm (P1515) to more than 2 000 ppm (W1030). For these cases where large differences can be seen (*e.g.* W1015), one should also observe related

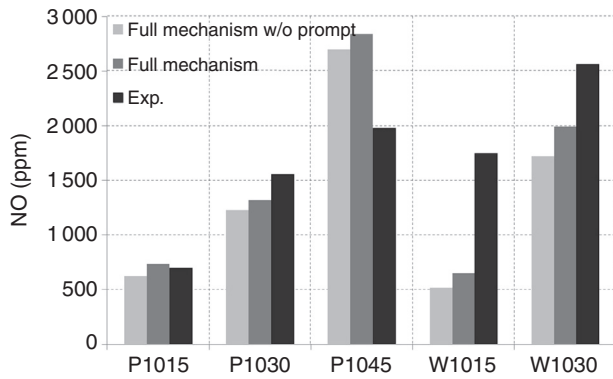


Figure 4
Comparison of measured and simulated NO molar fractions for stoichiometric combustion. Results without prompt mechanism are also included.

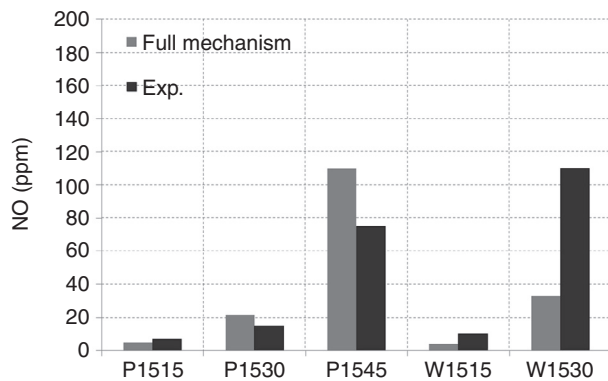


Figure 5
Comparison of measured and simulated NO molar fractions for lean ($\lambda = 1.5$) operating engine conditions.

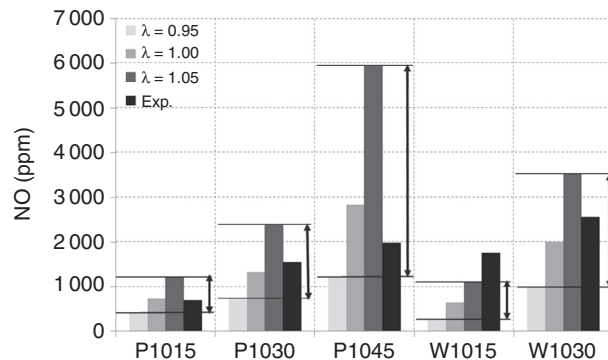


Figure 6
Impact of slight stoichiometry variation on NO_x formation.

differences in the thermodynamic data and not only in the reaction modeling. Cases with lower thermodynamic error show better prediction in NO_x results (example P1015). By using a more sophisticated combustion model [21, 22], the burning rate prediction could be improved with significant improvement in NO_x prediction as well.

As one might expect, the availability of oxygen is the key variable affecting NO_x prediction. This may be an additional reason of difference between measured and experimental data. Within a typical stoichiometric window of $[0.95 < \lambda < 1.05]$ that appears in actual engines during stoichiometric operation, slight differences in lambda could affect the total amount of NO_x formed during combustion. The stoichiometric cases of the experimental data were also simulated with a slightly rich ($\lambda = 0.95$) and slightly lean ($\lambda = 1.05$) mixture. The results are presented in Figure 6. It is observed that the measured NO_x concentration is almost always between these slightly lean and rich simulated values. Hence, slight departures from the set lambda in the experimental data may be a significant reason for the difference between experiment and simulation.

Figure 4 also shows that the “prompt” mechanism increases the total amount of NO_x concentrations by 10%-15% in case of stoichiometric combustion. Including the prompt formation one can increase the accuracy of the chemical mechanism. Bachmaier *et al.* (1973) [25] used an experimental configuration to define the equivalence ratio in which the prompt mechanism becomes significant in terms of total NO_x formation for various hydrocarbon mixtures. They found that the prompt NO formation starts to become significant as the mixture moves towards stoichiometry from $\lambda = 1.33$, in the case of methane. The prompt mechanism was negligible for leaner ($\lambda \geq 1.5$) conditions. Our results confirm the significance of the prompt mechanism in addition to the thermal one, even for stoichiometric combustion.

The thermodynamic input scenario is also important in lean conditions; however the oxygen availability does not affect the final results as much as in the stoichiometric case. In lean combustion, it seems that non-homogeneities in the burned zone can become important for accurately predicting final NO emissions. Multi-zoning is mostly used in 0D-engine models to take into account mixture stratification. In multi-zone modeling, different lambda and temperatures are assumed in each zone. Including multi-zones is a development we are currently working on in our model.

Another reason for differences between the simulated and experimental results could be the uncertainty in the high concentration of hydrocarbons (HC) that

this engine emits (up to 9 000 ppm). By assuming the measured concentration of HC in the model, the prompt mechanism appears very significant, even in the lean case. As this engine is an optical and not a production one, these HC were assumed to be generated from crevices in the piston/cylinder interface and oil oxidation, rather than from fuel combustion itself. Although these HC do not participate in combustion, they could have an effect in a cold outer zone of a multi-zone model.

4.2 Cycle-to-Cycle NO Variability

The detailed chemical mechanism was then used for the investigation of NO CCV. From the various engine points in Figure 4, four engine points were chosen for the CCV analysis; two in partial load (P1015, P1030) and two at wide open throttle operation (W1015, W1030). All engine points were selected in stoichiometric conditions, to also include the effect of the prompt mechanism in NO formation.

NO variability was investigated using a statistical analysis. Wiebe combustion parameters such as the ignition timing (SOI), the CD and the Wiebe shape coefficient (m) were randomly varied within limits, assuming that these parameters follow a normal distribution. The mean values for these distributions were equal to the values used in the case of mean cycle modeling. The range of the variation considered was taken from a relevant analysis in the framework of the FP6 LESS-CCV research project [29] and differed for partial load and WOT operation. Full load points correspond to higher CCV than low load engine points [2]. One hundred engine cycles were simulated in each engine point and the results of imep and NO_x concentrations are presented in distributions. Differences between mean cycle indices and CCV values are discussed.

4.2.1 Results of Cycle-to-Cycle Variation

Cycle-to-cycle variation of pressure and temperature are illustrated in Figures 7 and 8, respectively, for the engine point of partial load and ignition timing of 15° BTDC (P1015). The mean value of maximum pressure is 16.6 bar and the standard deviation is 0.98 bar, while the peak temperature has a mean value of 2 172 K and a standard deviation of 20 K.

Figures 9 and 10 illustrate the distributions of imep and NO concentration, respectively, for the same engine point (P1015), due to the variation of the combustion parameters. Both figures include the statistical characteristics of the distributions such as the mean value and the Standard Deviation (SD). Mean Cycle imep (MC imep)

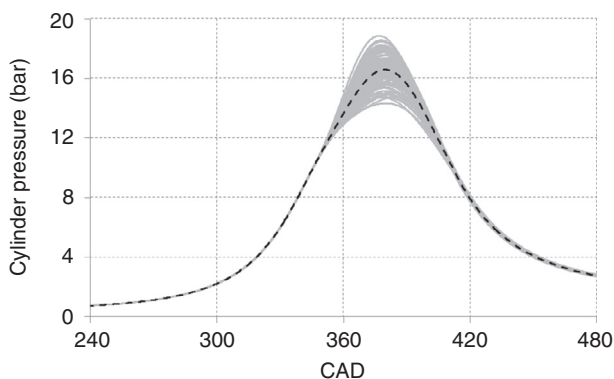


Figure 7
CCV of in-cylinder pressure (P1015 point).

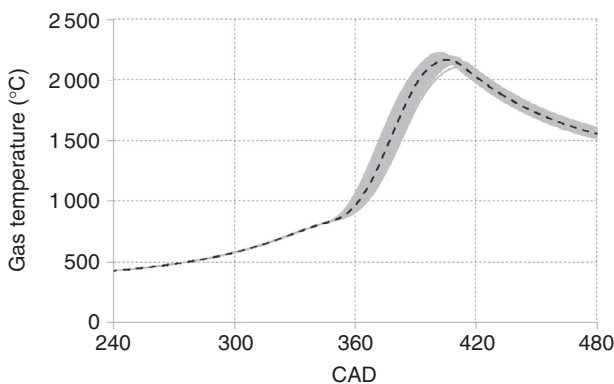


Figure 8
CCV of temperature evolution (P1015 point).

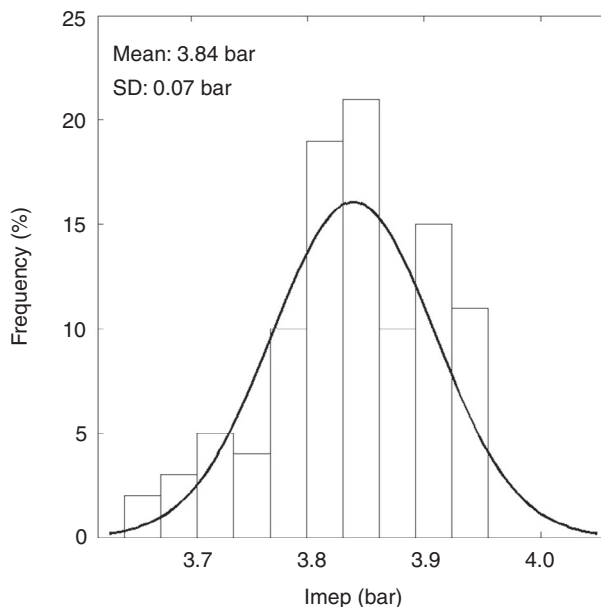


Figure 9
CCV of imep (P1015 point).

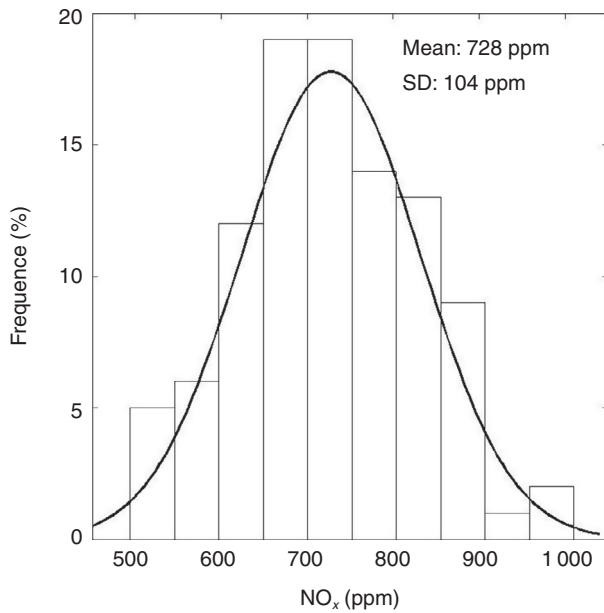


Figure 10
CCV NO_x (P1015 point).

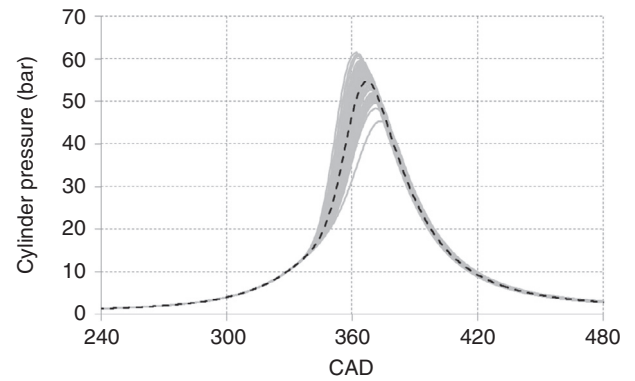


Figure 11
CCV of in-cylinder pressure (W1030 point).

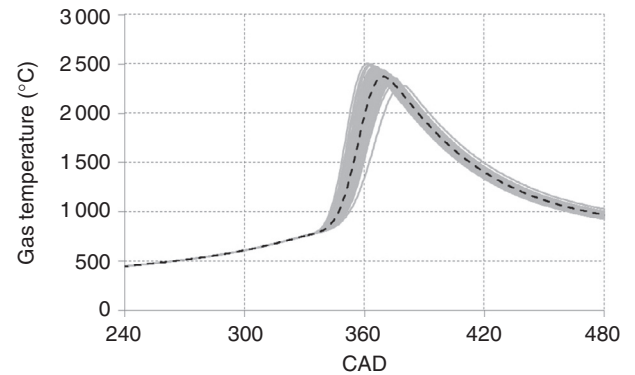


Figure 12
CCV of temperature evolution (W1030 point).

and the mean imep value of the CCV analysis coincide perfectly, while MC NO_x value and CCV mean NO_x value seems to have a slight deviation.

The same approach was also followed for the operation point at partial load (P1030) with ignition timing 30° BTDC. The peak pressure distribution has a mean value of 20.6 bar and the standard deviation is 1.05 bar. The peak temperature has a mean of 2 173 K and 30 K respectively. Distributions of this engine point for imep present no difference for the MC imep and the CCV imep value. In the case of NO, a small difference between MC NO_x and CCV NO_x values is again shown.

In the case of WOT, the same approach with a higher range of Wiebe parameters was used for the CCV analysis. Pressure and temperature plots of the engine point of 30° BTDC (W1030) are presented in Figures 11 and 12, respectively. Pressure and temperature peak values have a higher range as a result of higher range in the combustion parameters. In the case of W1015, the mean value of the maximum pressure is 35.7 bar and SD is equal with 3.1 bar, while the peak temperature varies from 2 121 K to 2 310 K with a mean value and standard deviation equal with 2 200 K and 39 K, respectively. Same order of magnitude differences are noticed for the case of W1030, where peak pressure varies from 45.5 bar to 61.7 bar (mean 55.5 bar, standard deviation

2.9 bar) and peak temperature varies from 2 281 K to 2 503 K (mean 2 410 K, standard deviation 42 K).

The distributions of imep and NO are illustrated in Figures 13 and 14. Due to higher CCV, MC imep and CCV imep are slightly different in both cases. Thus, MC NO_x value and CCV NO_x values present a higher deviation compared with the partial load. This also indicates that deviation between MC and CCV NO values is affected by the range of change of the combustion parameters.

4.2.2 Contribution of Prompt Mechanism on the Cycle-to-Cycle NO Variation

The impact of the prompt mechanism on NO_x CCV has been also investigated. In the case of mean cycle modeling, it was observed that the prompt mechanism accounts for an additional 10% to 15% in the final NO_x concentration. Therefore, it is expected that the

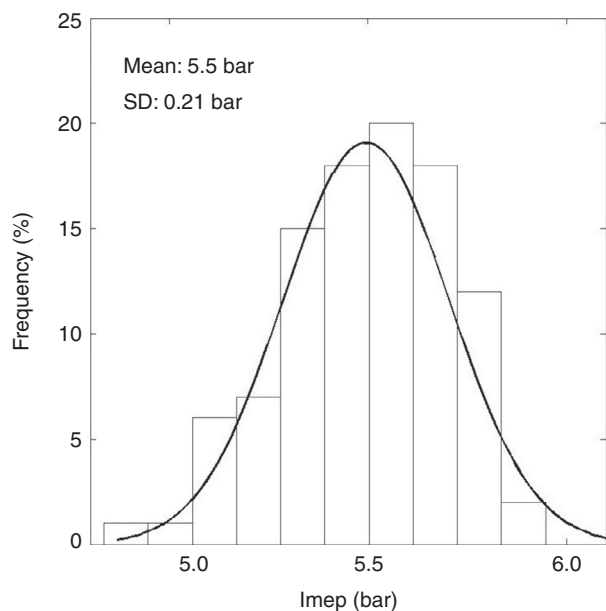


Figure 13
CCV of I_{mep} (W1030 point).

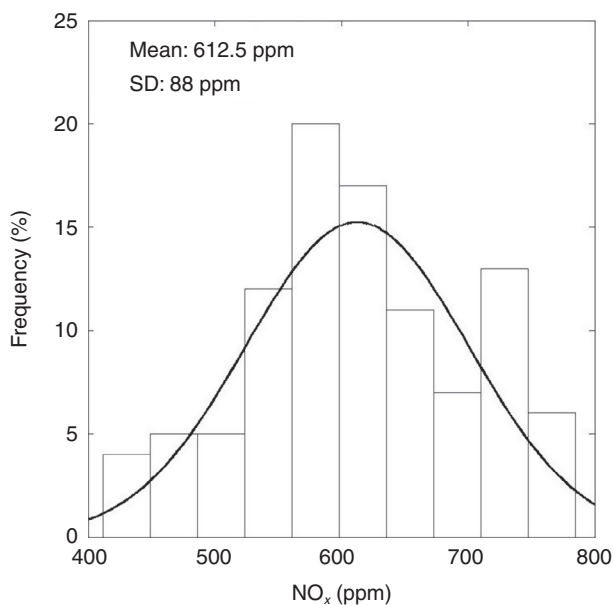


Figure 15
CCV NO_x without the prompt mechanism (P1015 point).

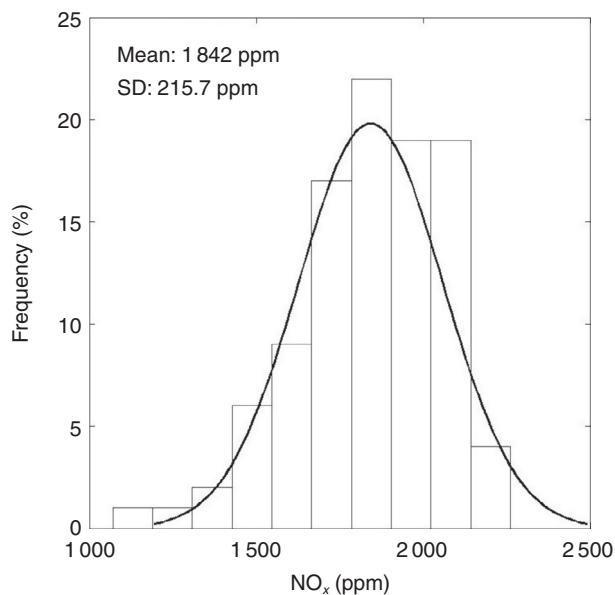


Figure 14
CCV NO_x (W1030 point).

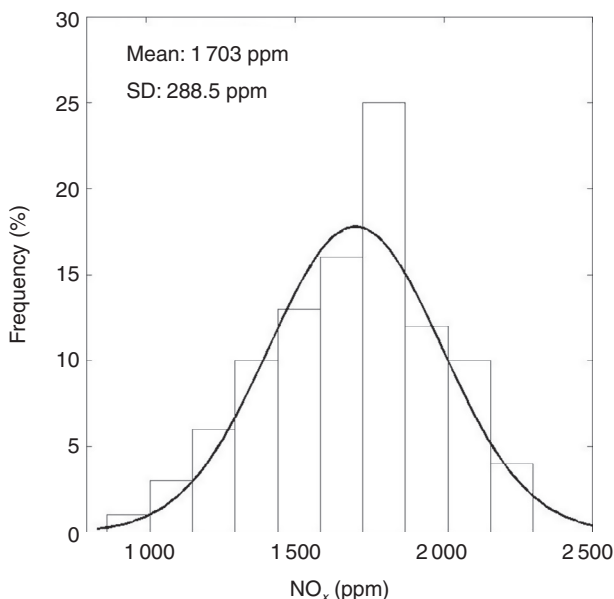


Figure 16
CCV NO_x without the prompt mechanism (W1030 point).

prompt mechanism should have a corresponding effect on NO CCV.

Figures 15 and 16 demonstrate the distributions of NO for a partial load and a full load engine point of CCV analysis, considering only the thermal mechanism.

Mean values of NO distribution show a decrease compared to the mean CCV NO values using the full mechanism. In addition, for the case of using the detailed chemical mechanism without the prompt one, a slight difference between MC NO values and CCV NO values

TABLE 4
Comparison of mean cycle values (MC) and CCV values for imep and NO

Engine point	Case	Imep (bar)	Diff (%)	NO full model (ppm)	Diff (%)	NO w/o prompt (ppm)	Diff (%)
P1015	MC	3.84	0.00	735	0.99	623	1.71
	CCV	3.84		728		613	
P1030	MC	3.27	0.00	1 320	0.65	1 230	4.14
	CCV	3.27		1 311		1 181	
W1015	MC	6.15	0.49	646	2.02	516	1.78
	CCV	6.12		633		507	
W1030	MC	5.55	0.90	1 990	8.05	1 720	0.97
	CCV	5.5		1 842		1 703	

is also observed. However, the prompt mechanism has an additional impact in the statistic characteristics of the NO distribution, which is described in the next section.

5 DEVIATION BETWEEN MEAN CYCLE VALUES AND MEAN CCV VALUES

CCV does not only result in a range of values for NO_x emissions but, due to the non-linearity of NO_x formation with combustion parameters and primarily with temperature, it may also have an impact on the average NO_x emitted. Hence, comparison between cycle-averaged values and the mean CCV value is important.

Partial load and full load are two cases that exhibit different variability for the combustion parameters. In partial load, the mean value of imep CCV distribution is almost the same to the mean cycle imep value. On the other hand, the CCV imep values are always lower than the mean cycle imep values in full load operation (Tab. 4). This means that the impact of CCV on average is a degradation of the engine performance.

NO formation is also affected by the variability in the combustion parameters. Both in full and partial load CCV NO_x values are always less than MC NO_x values, which reflects the CCV impact in NO formation (Tab. 4). In WOT operation, this impact is higher than in partial load. This result is related with the non-linearity of NO formation and for this reason it can not quantitatively correlated with imep variation. As shown in Table 4, the higher the difference between CCV imep and MC imep is, the higher is this difference between CCV NO_x and MC NO_x, too.

TABLE 5
Comparison of COV values for imep and NO with and without the prompt mechanism

Case	Imep COV (%)	NO full model COV (%)	NO w/o prompt COV (%)
P1015	1.81	14.30	14.35
P1030	0.84	14.50	13.77
W1015	0.81	26.03	26.89
W1030	3.81	11.71	16.94

The coefficient of variation is used as a metric of the intention of the NO CCV in Table 5. The impact of the prompt mechanism is also separated in this table. NO in general presents higher variability due to CCV than imep does. Also, the results show that it is not possible to establish a direct link between imep CCV and NO CCV. The latter is dependant on both the operation point and the CCV of imep. Finally, the impact of the prompt mechanism on CCV is also specific to the engine point considered. In one of the WOT conditions examined, the prompt mechanism led to a significant increase in NO CCV, that is not obvious in the other cases. This means that the combination of heat release rate with reaction kinetics is unique for each engine point that results to a behaviour which cannot be generalized at this stage. Simulations with other engines and further refinements in the model may lead to a more consistent behaviour of CCV NO with CCV in other combustion parameters.

CONCLUSIONS

In this study, a detailed chemical mechanism was used for the prediction of homogeneous engine-out NO emissions. Literature experimental data were used for the validation of the simulated values. The model satisfactorily predicts NO emissions, ranging from a few ppm to a couple of thousand of ppm of NO molar fraction, in both stoichiometric and lean conditions. Then, the model was used for the simulation of NO variation due to combustion CCV. It was found that CCV NO distributions exhibit a higher COV compared to the imep distributions. In addition, mean CCV NO values are always lower than the average cycle NO values. The impact of prompt mechanism in NO result was also investigated. In the case of average cycle emissions, it was found that the prompt mechanism increases the accuracy of the prediction, especially in stoichiometric conditions by up to 15%. In CCV, the prompt mechanism has an impact in the COV and mean value of NO distributions, although the impact was dependant on the engine operation point considered.

ACKNOWLEDGMENTS

This study was performed within the framework of the FP7 LESSCCV research project (Grant agreement 233615).

REFERENCES

- Brehob D.D., Newman C.E. (1992) Monte Carlo Simulation of Cycle by Cycle Variability, *SAE Paper* 922165.
- Ozдор N., Dulger M., Sher E. (1994) Cyclic Variability in Spark Ignition Engines. A Literature Survey, *SAE Paper* 940987.
- Karvountzis-Kontakiotis A., Ntziachristos L. (2012) A detailed chemical mechanism to predict NO cycle-to-cycle variation in homogeneous engine combustion, *IFAC Workshop on Engine and Powertrain Control, Simulation and Modeling*, IFP Energies nouvelles, France, 23-25 Oct.
- Ball J.K., Raine R.R., Stone C.R. (1998) Combustion analysis and cycle-by-cycle variations in spark ignition engine combustion Part 2: A new parameter for completeness of combustion and its use in modelling cycle-by-cycle variations in combustion, *Proceeding of the Institution of Mechanical Engineers, Part D: Journal of Automobile Engineering June 1* **212**, 6, 507-523.
- Heywood J.B. (1988) *Internal Combustion Engine Fundamentals*, McGraw-Hill, Singapore.
- Young M.B. (1981) Cyclic Dispersion in the Homogeneous-Charge Spark-Ignition - A Literature Survey, *SAE Paper* 810020.
- Stone C.R., Brown A.G., Beckwith P. (1996) Cycle-by-Cycle Variations in Spark Ignition Engine Combustion – Part II: Modelling of Flame Kernel Displacements as a Cause of Cycle-by-Cycle Variations, *SAE Paper* 960613.
- Johansson B. (1996) Cycle-to-Cycle Variations in S.I. Engines – The Effects of Fluid Flow and Gas Composition in the Vicinity of the Spark Plug on Early Combustion, *SAE Paper* 962084.
- Whitelaw J.H., Xu H.M. (1995) Cyclic Variations in a Lean-Burn Spark Ignition Engine Without and With Swirl, *SAE Paper* 950683.
- Fox W.J., Cheng K.W., Heywood B.J. (1993) A Model for Predicting Residual Gas Fraction in Spark-Ignition Engines, *SAE Paper* 931025.
- Hamai K., Kawajiri H., Ishizuka T., Nakai M. (1988) Combustion Fluctuation Mechanism Involving Cycle-to-Cycle Spark Ignition Variation Due to Gas Flow Motion in S.I. Engines, *21st Int. Symposium on Combustion* **21**, 505-512.
- Vermorel O., Richard S., Colin O., Angelberger C., Benkenida A., Veynante D. (2009) Towards the understanding of cyclic variability in a spark ignited engine using multi-cycle LES, *Combustion and Flame* **156**, 1525-1541.
- Lacour C., Pera C. (2011) An Experimental Database Dedicated to the Study and Modelling of Cyclic Variability in Spark-Ignition Engines with LES, *SAE Paper* 2011-01-1282.
- Martin J., Witze P., Borgnakke C. (1985) Combustion Effects on the Pre-flame Flow Field in a Research Engine, *SAE Paper* 850122.
- Matekunas F. (1983) Modes and Measures of Cyclic Combustion Variability, *SAE Paper* 830337.
- Shen H., Hinze P., Heywood J. (1996) A Study of Cycle-to-Cycle Variations in SI Engines Using a Modified Quasi-Dimensional Model, *SAE Paper* 961187.
- Watson C.H., Goldsworthy C.L., Milkins E.E. (1976) Cycle-by-Cycle Variations of HC, CO, and NOx, *SAE Paper* 760753.
- Ball K.J., Bowe J.M., Stone C.R., Collings N. (2001) Validation of a Cyclic NO Formation Model with Fast NO Measurements, *SAE Paper* 2001-01-1010.
- Jante A. (1960) Das Wiebe-Brenngesetz; ein Fortschritt in der Thermodynamik der Kreisprozesse von Verbrennungsmotoren, *Kraftfahrzeugtechnik* **9**, 340-346.
- Stiesch G. (2003) *Modeling Engine Spray and Combustion Processes*, Springer, Berlin.
- Duclos J.-M., Zolver M., Baritaud T. (1999) 3D Modeling of Combustion for DI-SI Engines, *Oil & Gas Science and Technology* **54**, 2, 259-264.
- Richard S., Bougrine S., Font G., Lafossas F.-A., Le Berr F. (2009) On the Reduction of a 3D CFD Combustion Model to Build a Physical 0D Model for Simulating Heat Release, Knock and Pollutants in SI Engines, *Oil & Gas Science and Technology* **64**, 3, 223-242.
- Heywood J.B., Higgins J.M., Watts P.A., Tabaczynski R.J. (1979) Development and Use of a Cycle Simulation to Predict SI Engine Efficiency and NOx Emissions, *SAE Paper* 790291.
- Pattas K., Häfner G. (1973) Stichoxydbildung bei der otto-motorischen Verbrennung, *MTZ*, Nr. 12.

- 25 Bachmaier F., Eberius K.H., Just T.H. (1973) The formation of Nitric Oxide and the Detection of HCN in Premixed Hydrocarbon – Air Flames at 1 Atmosphere, *Combustion Science and Technology* **7**, 77-84.
- 26 Lutz A.E., Kee R.J., Miller J.A. (1988) Senkin: A FORTRAN program for predicting homogeneous gas phase chemical kinetics with sensitivity analysis, SAND87-8248.
- 27 Glassman I., Richard A.Y. (2008) *Combustion*, Academic Press, California, USA.
- 28 Kergin U. (2002) Study on the prediction of the effects of design and operating parameters on NO_x emissions from a leanburn natural gas engine, *Energy Conversion and Management* **44**, 907-921.
- 29 Shuemie A., Fairbrother R., Pötsch Ch, Tatschl R. (2011) *LESSCCV Project Meeting*, Milano, WP4.
- 30 Merker G.P., Schwarz C., Stiesch G., Otto F. (2004) *Simulation of combustion and pollutant formation for engine-development*, Springer.

Manuscript accepted in October 2013

Published online in March 2014